Alternative quinone substrates and inhibitors of human electron-transfer flavoprotein-ubiquinone oxidoreductase

Martin ŠIMKOVIČ* and Frank E. FRERMAN*†[1]

*Department of Pediatrics, University of Colorado Health Sciences Center, Denver, CO 80262, U.S.A., and †Department of Pharmaceutical Sciences, University of Colorado Health Sciences Center, Denver, CO 80262, U.S.A.

Electron-transfer flavoprotein (ETF)-ubiquinone (2,3-dimethoxy-5-methyl-1,4-benzoquinone) oxidoreductase (ETF-QO) is a membrane-bound iron–sulphur flavoprotein that participates in an electron-transport pathway between eleven mitochondrial flavoprotein dehydrogenases and the ubiquinone pool. ETF is the intermediate electron carrier between the dehydrogenases and ETF-QO. The steady-state kinetic constants of human ETF-QO were determined with ubiquinone homologues and analogues that contained saturated n-alkyl substituents at the 6 position. These experiments show that optimal substrates contain a ten-carbon-atom side chain, consistent with a preliminary crystal structure that shows that only the first two of ten isoprene units of co-enzyme Q_{10} (CoQ_{10}) interact with the protein. Derivatives with saturated alkyl side chains are very good substrates, indicating that, unlike other ubiquinone oxidoreductases, there is little preference for the methyl branches or rigidity of the CoQ side chain. Few of the compounds that inhibit ubiquinone oxidoreductases inhibit ETF-QO. Compounds found to act as inhibitors of ETF-QO include 2-*n*-heptyl-4-hydroxyquinoline *N*-oxide, a naphthoquinone analogue, 2-(3-methylpentyl)-4,6-dinitrophenol and pentachlorophenol. 2,5-Dibromo-3-methyl-6-isopropyl-*p*-benzoquinone (DBMIB), which inhibits the mitochondrial bc_1 complex and the chloroplast b_6f complex in redox-dependent fashion, can serve as an electron acceptor for human ETF-QO. The observation of simple Michaelis–Menten kinetic patterns and a single type of quinone-binding site, determined by fluorescence titrations of the protein with DBMIB and 6-(10-bromodecyl)ubiquinone, are consistent with one ubiquinone-binding site per ETF-QO monomer.

Key words: acyl-CoA dehydrogenase, electron-transfer flavoprotein, electron-transfer flavoprotein-ubiquinone oxidoreductase, naphthoquinone.

INTRODUCTION

Electron-transfer flavoprotein (ETF)-ubiquinone (2,3-dimethoxy-5-methyl-1,4-benzoquinone) oxidoreductase (ETF-QO) is a mitochondrial enzyme that catalyses electron transfer from ETF to co-enzyme Q (CoQ) in the mitochondrial respiratory chain. It is an integral membrane protein (approx. 64 kDa) containing one equivalent of FAD and a $[4Fe–4S]^{2+,1+}$ cluster, and is one of the simplest quinone oxidoreductases in the respiratory chain [1–3]. The protein serves as the input site to the main respiratory chain for reducing equivalents derived from the nine acyl-CoA dehydrogenases and two N-methyl dehydrogenases [1–3]. Human and porcine ETF-QOs appear to function as monomers, and only a single equivalent of ubiquinone per monomer is observed in a preliminary crystal structure of the porcine protein [4]. The observation of a single type of ubiquinone-binding site is consistent with the data of Watmough et al. [5] who studied porcine ETF-QO. They investigated the binding of a brominated alternative substrate, 6-(10-bromodecyl)ubiquinone, by fluorimetric titration of the porcine protein. Several water-soluble ubiquinone homologues have been investigated as substrates for human ETF-QO [6]. The optimum side chain in the latter investigation was determined to be ten carbon atoms, and the turnover of human ETF-QO with the isoprenalogue, Q_2 (ubiquinone carrying a side chain of two isoprene units at the 6 position), is similar to that of decyl-ubiquinone that has an n-alkyl side chain. The K_m for Q_2 is somewhat less than the K_m for the decyl analogue [6]. The three-dimensional structure shows that only the first two isoprene units of Q_{10} are bound to the protein, and the third to tenth isoprene units remain in the membrane phase [4]. The question of the intramolecular electron-transport pathway and the mechanism of ubiquinone reduction are complicated by the preliminary three-dimensional structure of Kim et al. [4]. Based on the oxidation–reduction potentials of the FAD, iron–sulphur and ubiquinone, it had been assumed that electrons from ETF enter ETF-QO through the flavin ($E_0' = +28$ mV, semiquinone/oxidized couple) and are transferred to the cluster ($E_0' = +47$ mV), which is the immediate reductant of ubiquinone ($E_0' \approx +100$ mV) [7]. However, the minimum distance between the cluster and the 1,4-benzoquinone head group is 19 Å (1 Å = 0.1 nm), making it unlikely that the cluster is the immediate reductant of ubiquinone [4]. In contrast, the isoalloxazine–benzoquinone distance is 8.5 Å, which would be favourable for electron transfer [8]. In the investigations reported in the present paper, we have focused on the ubiquinone site, using alternative substrates and quinone analogues and inhibitors that could serve as useful structural and mechanistic probes.

Abbreviations used: carboxin, 5,6-dihydro-2-methyl-1,4-oxathi-ine-3-carboxanilide; CoQ, co-enzyme Q; DBMIB, 2,5-dibromo-3-methyl-6-isopropyl-*p*-benzoquinone; DTT, dithiothreitol; duroquinone, 2,3,5,6-tetramethyl-*p*-benzoquinone; ETF, electron-transfer flavoprotein; ETF-QO, ETF-ubiquinone oxidoreductase; HNNQ, 2-hydroxy-3-*n*-nonyl-1,4-naphthoquinone; HOQNO, 2-*n*-heptyl-4-hydroxyquinoline *N*-oxide; IDNP, 2-isopropyl-4,6-dinitrophenol; lapachol, 2-hydroxy-3-(3-methyl-2-butenyl)-1,4-naphthoquinone; MCAD, medium-chain acyl-CoA dehydrogenase; menadione, 2-methyl-1,4-naphthoquinone (vitamin K_3); MPDNP, 2-(3-methylpentyl)-4,6-dinitrophenol; PCP, 2,3,4,5,6-pentachlorophenol; pyridaben, 2-tert-butyl-5-(4-tert-butylbenzylthio)-4-chloropyridazin-3(2H)-one; Q_n, ubiquinone carrying a side chain of *n* isoprene units at the 6 position; ubiquinone, 2,3-dimethoxy-5-methyl-1,4-benzoquinone.

[1] To whom correspondence should be addressed, at 4200 E. Ninth Ave., Department of Pediatrics, Box C233, Denver, CO 80262, U.S.A. (e-mail frank.frerman@uchsc.edu).

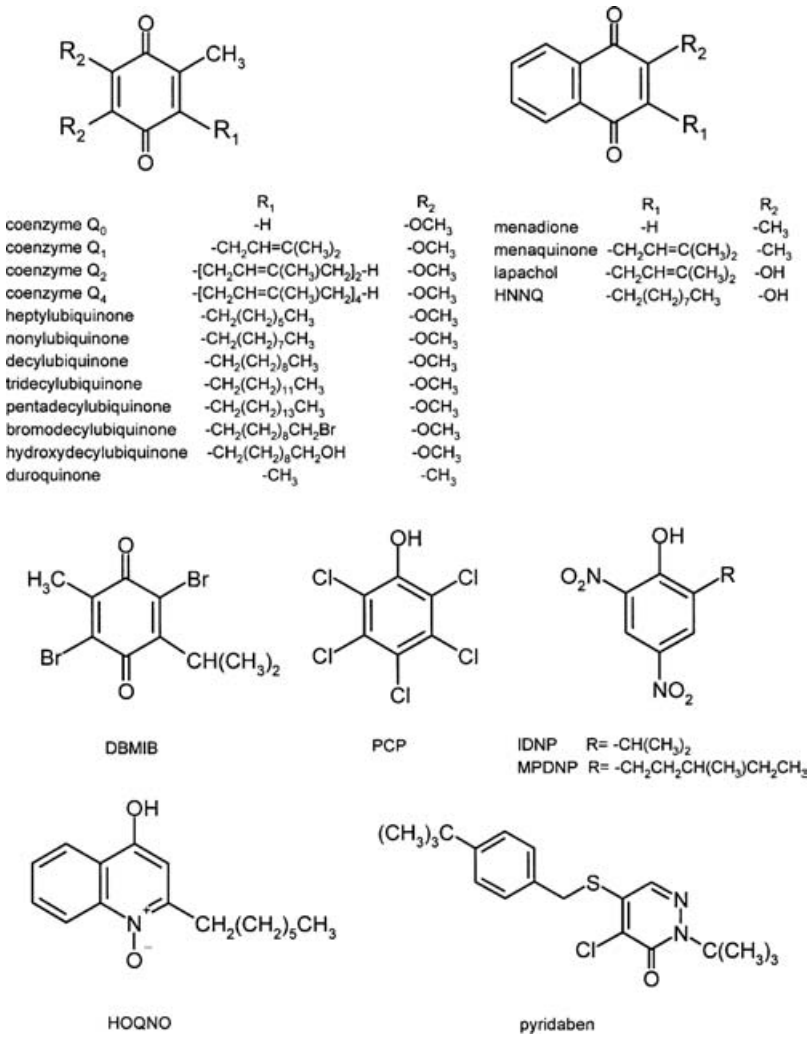

Figure 1 Structures of the quinone alternative substrates and inhibitors used in this investigation

EXPERIMENTAL

Materials

The quinone substrates, Q_1 (ubiquinone carrying a side chain of one isoprene unit at the 6 position), Q_2, duroquinone (2,3,5,6-tetramethyl-*p*-benzoquinone), menadione [2-methyl-1,4-naphthoquinone (vitamin K_3)] and the inhibitors, HOQNO (2-*n*-heptyl-4-hydroxyquinoline *N*-oxide), DBMIB (2,5-dibromo-3-methyl-6-isopropyl-*p*-benziquinone), antimycin A and rotenone were purchased from Sigma Chemical Co. (St. Louis, MO, U.S.A.). PCP (2,3,4,5,6-pentachlorophenol), atrazine [6-chloro-*N*-ethyl-*N*′-(1-methylethyl)-1,3,5-triazine-2,4-diamine], lapachol [2-hydroxy-3-(3-methyl-2-butenyl)-1,4-naphthoquinone] and HNNQ (2-hydroxy-3-*n*-nonyl-1,4-naphthoquinone) were from Aldrich Chemical Co. (Milwaukee, WI, U.S.A.). Myxothiazole was purchased from Fluka (Milwaukee, WI, U.S.A.). Carboxin (5,6-dihydro-2-methyl-1,4-oxathi-ine-3-carboxanilide) was purchased from Chem Service Inc. (West Chester, PA, U.S.A.). The 2-substituted-4,6-dinitrophenols, IDNP (2-isopropyl-4,6-dinitrophenol) and MPDNP [2-(3-methylpentyl)-4,6-dinitrophenol], were synthesized and generously given to us by Dr Hideto Miyoshi (Department of Agricultural Chemistry, Kyoto University, Kyoto, Japan). Pyridaben [2-tert-butyl-5-(4-tert-butylbenzylthio)-4-chloropyridazin-3(2H)-one] was a gift from BASF Corporation (Research Triangle Park, NC, U.S.A.). Menaquinone-1 was a gift from Eisai Co. (Tokyo, Japan). The ubiquinone analogues with n-alkyl substitutions at the 6 position of the quinone ring were gifts from Dr Bernard Trumpower (Department of Biochemistry, Dartmouth Medical School, Hanover, NH, U.S.A.). The terminally substituted analogues, 6-(10-hydroxydecyl)- and 6-(10-bromodecyl)-ubiquinone, were synthesized as described by Yu and Yu [9]. The structures of the quinone substrates and inhibitors used in this work are shown in Figure 1.

Other chemicals were from commercial sources and were the best grade available.

Purification of enzymes

Human ETF-QO was expressed in Sf9 cells using a baculovirus vector and was purified as previously described [6] with a single modification of the purification procedure. Chromatography on Q Sepharose™ Fast Flow (5 × 5 ml) replaced the chromatography step on hydroxyapatite Ultrogel. The Q Sepharose™ column was equilibrated with 20 mM Tris/HCl buffer (pH 7.4) containing 24 mM β-*n*-octyl D-glucoside and 0.1 mM DTT (dithiothreitol). The protein, dialysed against the same buffer, was loaded on to the column, which was then washed with 125 ml of the equilibration buffer. Human ETF-QO was eluted with a 200 ml

linear gradient from 0.24 to 0.48 M KCl in 20 mM Tris/HCl containing 24 mM β-*n*-octyl D-glucoside and 0.1 mM DTT. Human ETF and human medium-chain acyl-CoA dehydrogenase (MCAD) were expressed from pET vectors in *Escherichia coli* and purified as previously described [10,11].

Enzyme assays

ETF-QO was assayed as a ubiquinone reductase in the reaction mixtures containing 50 mM Hepes-K^+, pH 7.4, 1 μM human MCAD, 1 μM human ETF, 100 μM octanoyl-CoA, 6 mM CHAPS and 60 μM CoQ_1 at 25 °C. The reaction was initiated by the addition of ETF-QO and monitored as the decrease in absorbance at 275 nm ($\Delta\varepsilon_{275} = 7.4 \times 10^3\ M^{-1} \cdot cm^{-1}$) due to the reduction of ubiquinone to the dihydroquinone [5,12].

Steady-state kinetics

When the steady-state kinetic constants for quinone reduction were determined, concentrations of the human MCAD and human ETF were increased to saturating concentrations (3 μM). All quinone stocks were prepared in ethanol. The rates of quinone reduction were calculated using the oxidized–reduced difference molar absorption coefficients, which take into account the change in absorbance in the region that results from the oxidation of octanoyl-CoA to 2-octenoyl-CoA. These difference molar absorption coefficients were determined as previously described [5,12]. The following difference molar absorption coefficients were used: $\Delta\varepsilon_{270} = 13.1\ mM^{-1} \cdot cm^{-1}$ for duroquinone, and $\Delta\varepsilon_{262} = 9.3\ mM^{-1} \cdot cm^{-1}$ for menadione. The values of $\Delta\varepsilon_{278}$ for the 6-(10-decyl)ubiquinone derivatives were as previously reported [5] and a value of $\Delta\varepsilon_{278} = 7.6\ mM^{-1} \cdot cm^{-1}$ was used for the saturated 6-*n*-alkyl ubiquinone analogues.

Steady-state kinetic constants and their standard errors were determined by non-linear least squares fit of the data to the Michaelis–Menten equation using Origin 6.1 software (OriginLab Corporation, Northampton, MA, U.S.A.).

Inhibition of ETF-QO

Inhibition constants for selected inhibitors were determined at fixed, varied concentrations of the inhibitors and varied concentrations of Q_1 in the assay system described above. The final concentration of ethanol or DMSO, the solvents for inhibitors and for Q_1, did not exceed 1 % (v/v) in the assays. The data were analysed by non-linear least squares fits to equations describing different inhibition models: uncompetitive [eqn (1)], non-competitive [eqn (2)], competitive [eqn (3)] and hyperbolic mixed type [eqn (4)] using Grafit 4.0 software (Erithacus Software, Horley, Surrey, U.K.).

$$v = \frac{v_{max} \cdot [S]}{K_m + [S] \cdot \left(1 + \frac{[I]}{K_i}\right)} \quad (1)$$

$$v = \frac{v_{max} \cdot [S]}{K_m \cdot \left(1 + \frac{[I]}{K_i}\right) + [S] \cdot \left(1 + \frac{[I]}{K_i}\right)} \quad (2)$$

$$v = \frac{v_{max} \cdot [S]}{K_m \cdot \left(1 + \frac{[I]}{K_i}\right) + [S]} \quad (3)$$

$$v = \frac{v_{max} \cdot [S]}{K_s \cdot \frac{\left(1 + \frac{[I]}{K_i}\right)}{\left(1 + \frac{\beta[I]}{\alpha K_i}\right)} + \frac{\left(1 + \frac{[I]}{\alpha K_i}\right)}{\left(1 + \frac{\beta[I]}{\alpha K_i}\right)}} \quad (4)$$

In these equations, v is the initial velocity, v_{max} is the maximal velocity, K_m is the Michaelis–Menten constant, K_i is the inhibition constant, [S] is the substrate concentration, [I] is the inhibitor concentration, α is the factor by which K_i or K_s changes when substrate or inhibitor is bound to the enzyme and β is the factor by which the catalytic constant changes when inhibitor is bound to the enzyme [13].

Fluorimetric determination of K_d

The K_d of the DBMIB–ETF-QO complex was determined by fluorimetric titration of the human enzyme with DBMIB at 25 °C. Human ETF-QO in 0.8 ml of 100 mM Hepes buffer (pH 7.4) containing 6 mM CHAPS was titrated with DBMIB. Binding of DBMIB to human ETF-QO was detected as the decrease in fluorescence emission intensity at 330 nm when excited at 280 nm. DBMIB was added from stock solutions in 40 % ethanol and the final concentration of ethanol never exceeded 5 % in the titration mixtures. This concentration had no effect on protein fluorescence. Data were corrected for dilution, and for inner filter effect. Correction for the inner filter effect due to DBMIB and protein was made using the equation [14]:

$$F_{con} = F_{obs} \cdot \text{antilog}[(A_{ex} + A_{em})/2]$$

where F_{obs} is the observed emission intensity of human ETF-QO corrected for background, F_{corr} is the emission intensity corrected for inner filter effect, A_{ex} and A_{em} are the absorbance of the human ETF-QO and DBMIB mixtures at the excitation and emission wavelengths respectively. The K_d of DBMIB binding was determined by non-linear fitting of the data to the ligand-binding equation by Origin version 6.1 software:

$$\chi = n[DBMIB]_{free}/(K_d + [DBMIB]_{free})$$

where χ is fractional saturation of human ETF-QO. This parameter was calculated from $(F_o - F)/(F_o - F_{max})$, where F, F_o and F_{max} are the corrected fluorescence intensities of human ETF-QO in the presence, absence and under saturating concentrations of DBMIB, K_d is the dissociation constant and n is the maximal saturation. $[DBMIB]_{free}$ was calculated by:

$$[DBMIB]_{free} = [DBMIB]_{total} - \chi \cdot [ETF\text{-}QO]_{total}$$

where $[DBMIB]_{total}$ is the total concentration of DBMIB in the sample and $[ETF\text{-}QO]_{total}$ is the total concentration of human ETF-QO (both concentrations after correction for dilution) [15].

Other methods

Anaerobic reduction of ETF-QO and ETF were carried out photochemically in the presence of 5-deazaflavin at 4 °C as previously described [16].

Protein concentration was determined by the Bradford method with BSA as a standard [17]. The concentration of purified ETF-QO was estimated by using $\varepsilon_{430} = 24 \times 10^3\ M^{-1} \cdot cm^{-1}$ [6].

RESULTS AND DISCUSSION

Alternative quinone substrates

Table 1 shows the steady-state kinetic constants of human ETF-QO for Q_1, Q_2 and several 6-alkyl derivatives of ubiquinone. For reference, the table also shows kinetic constants for Q_4

Table 1 Steady-state kinetic constants of human ETF-QO with ubiquinone homologues and analogues

Varied substrate	k_{cat} (s^{-1})	K_m (μM)	k_{cat}/K_m ($\mu M^{-1} \cdot s^{-1}$)
Q_1	34.5 ± 0.9	9.5 ± 0.7	3.6
Q_2	68.7 ± 1.8	6.9 ± 0.5	10.0
Q_4*	35.5 ± 1.3	14.8 ± 1.4	2.4
Heptylubiquinone	54.0 ± 1.3	8.2 ± 0.6	6.6
Nonylubiquinone	61.3 ± 1.5	7.3 ± 0.7	8.4
Decylubiquinone	59.9 ± 1.9	7.9 ± 0.9	7.5
Tridecylubiquinone	31.5 ± 3.3	26.5 ± 3.8	1.2
Pentadecylubiquinone	7.4 ± 0.32	2.3 ± 2.3	0.3
Bromodecylubiquinone	60.8 ± 3.9	8.9 ± 0.8	6.8
Hydroxydecylubiquinone	67.0 ± 2.1	9.9 ± 0.8	6.7
Duroquinone	18.1 ± 0.8	19.5 ± 2.1	0.9
Menadione	6.6 ± 0.4	16.3 ± 1.9	0.4

* Taken from Šimkovič et al. [6].

that were determined previously [6]. Q_2 is the optimal substrate among readily available water-soluble analogues that have been examined, as judged by the value of k_{cat}/K_m in the present study and a previous study [6]. There appears to be no strict requirement for the methyl branch or the rigidity of the isoprene structure. Rather, the binding of the side chain appears to be dependent on the number of carbon atoms, with the optimum being a nine- or ten-carbon-atom side chain. Substitution of the polar hydroxy group or apolar bromine atom at C-10 of the decyl side chain results in no significant change on binding or the turnover of the enzyme. These substituents have about the same size as a methyl group. When the number of carbon atoms in the n-alkyl chain exceeds ten, the binding and turnover of the enzyme declines, following the decline in activity with Q_4. Although solubility may be a problem with Q_4 [6], solubility does not appear to be a problem with 6-tridecylubiquinone. Duroquinone and menadione were also investigated as alternative substrates. Duroquinone and the naphthoquinone, menadione (vitamin K_3), are substrates of ETF-QO. Since reduced menadione reacts with oxygen, the steady-state kinetic experiments were conducted under anaerobic conditions. The turnover numbers of ETF-QO with duroquinone and menadione are 22% and 8% respectively of that of Q_2. Neither of these quinones react directly with reduced ETF. This is important for interpretation of the steady-state kinetic results because ETF semiquinone, but not the dihydroquinone form of ETF, is able to reduce ubiquinone directly [12]. Similarly, the low potential, reduced naphthoquinones, menaquinol-1 ($E_0' = -74$ mV [18]) and lapachol ($E_0' = -155$ mV [19]), reduce ETF directly. The decreased values of k_{cat} with duroquinone and menadione probably result from the lower potentials $E_0' = +5$ mV and $E_0' = -13$ mV respectively. The K_m values of the alternative substrates are only 3- to 4-fold greater than that of Q_2. Therefore the quinone site of human ETF-QO is able to bind naphthoquinones as well as benzoquinones as indicated by the reduction of menadione. Also, the longer side chain is not absolutely required since duroquinone functions as a substrate.

DBMIB is a ubiquinone analogue that is an inhibitor of the chloroplast cytochrome b_6f and mitochondrial bc_1 complexes [20–23]. It is redox-active and its inhibitory activity is dependent on the redox poise of the complexes [24]. Although the potentials are favourable, neither Q_0 ($E_0' \approx +90$ mV) nor DBMIB ($E_0' = +180$ mV [25]) could be used as substrates because they are reduced by both semiquinone and dihydroquinone oxidation states of ETF (results not shown). ETF semiquinone is reoxidized with a stoichiometry of approx. 0.41 mol of DBMIB per mol of ETF flavin, and 1.14 mol of DBMIB are reduced per mol of ETF dihydroquinone. DBMIB can serve also as an electron acceptor for human ETF-QO. Figure 2 shows an oxidative titration of two-electron and three-electron reduced forms of ETF-QO by DBMIB under anaerobic conditions. The reoxidation of two-electron and three-electron reduced forms of ETF-QO by DBMIB has a stoichiometry of 0.98 and 1.40 mol of DBMIB per mol of ETF-QO respectively.

The binding of DBMIB to human ETF-QO could be monitored by quenching of tryptophan fluorescence. Similar experiments were carried out by Watmough et al. [5] with 6-(10-bromodecyl)-ubiquinone. Analysis of the data shown in Figure 3 yields a K_d of 0.23 ± 0.05 μM. By way of comparison, the binding constant

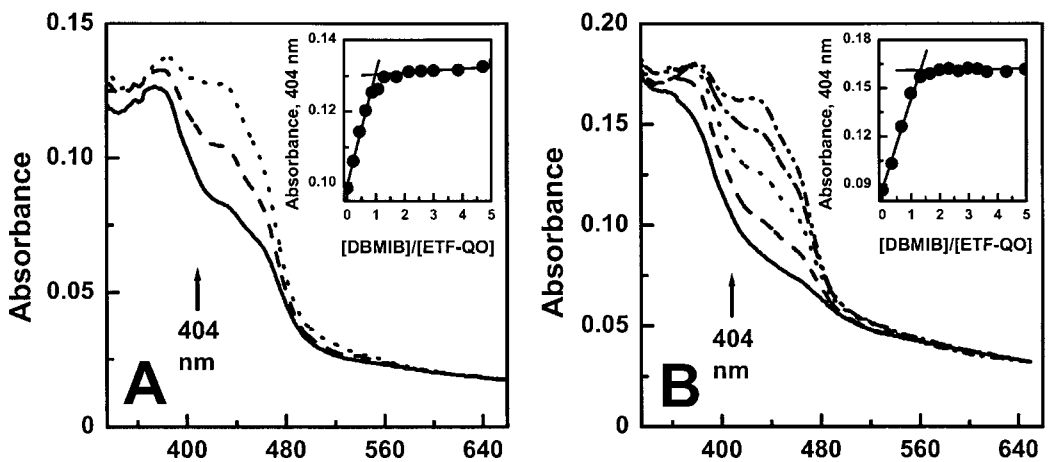

Figure 2 Titration of two-electron reduced (A) and three-electron reduced (B) human ETF-QO with oxidized DBMIB under anaerobic conditions

The reaction mixtures contained human ETF-QO in 50 mM Hepes buffer, pH 7.4, 2 mM EDTA, 6 mM CHAPS, 1.25 μM 5-deazaflavin and 30 mM glucose. The cuvettes were sealed with silicone rubber septa, evacuated and purged with argon; residual oxygen was removed by addition of glucose oxidase/catalase [6]. ETF-QO was reduced photochemically by illumination and the extent of ETF-QO reduction was monitored spectrophotometrically. The reduced protein was then titrated with DBMIB dissolved in 40% (v/v) ethanol containing 50 mM Hepes buffer and 6 mM CHAPS. The curves of absorbance spectra in the main plot correspond to molar ratios of [DBMIB]/[ETF-QO] as follows: 0 (——), 0.5 (----) and 1 (·····) (**A**); and 0 (——), 0.3 (----), 0.7 (·····), 1 (-·-·-) and 1.5 (-··-··) (**B**). The insets show the increase in absorbance at 404 nm as a function of [DBMIB]/[ETF-QO]. The absorbance at 404 nm was obtained from the absorption spectra. Data were corrected for dilution and some spectra are omitted for clarity.

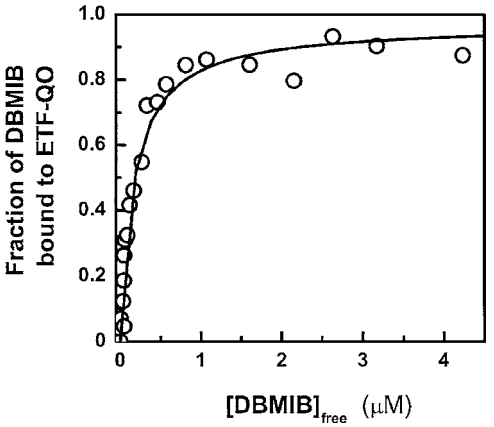

Figure 3 Fluorimetric titration of human ETF-QO with DBMIB

Oxidized human ETF-QO (0.6 μM) was titrated with DBMIB and the quenching of fluorescence was determined as a function of DBMIB concentration at 25 °C. The protein was excited at 280 nm and emission at 332 nm was monitored. Spectra were corrected for dilution and inner filter effect.

for the 6-(10-bromodecyl)-ubiquinone analogue is 2.2 μM. These K_d values are somewhat lower than the dissociation constants for a range of ubiquinone homologues and inhibitors with the bc_1 complex from beef heart [26].

The low potentials of the naphthoquinones, menaquinone and lapachol, render them inactive as substrates for the reoxidation of ETF-QO, and because these naphthoquinols reduce ETF directly, it was not possible to monitor the reverse reaction, i.e. ETF reduction catalysed by ETF-QO. However, both quinones reduce ETF-QO stoichiometrically (Figure 4). Complete reduction by menaquinol required 1.67 mol per mol of ETF-QO and full reduction by lapachol required 1.52 mol per mol of ETF-QO.

The experiments with alternative quinone substrates of ETF-QO demonstrate several important points regarding the quinone site in the protein and its relationship to other binding sites in quinone oxidoreductases. The demonstration of simple Michaelis–Menten steady-state kinetic patterns is consistent with a single quinone-binding site in pig and human ETF-QO [5,6]. Furthermore, both mammalian proteins appear to have a single type of quinone-binding site as judged by binding of two different brominated alternative quinone substrates. These data are important because they appear to rule out a second quinone-binding site at which a second quinone molecule could be reduced by the iron–sulphur cluster. The cluster–quinone distance is 19 Å [4], which is greater than 14 Å, the apparent upper limit for direct electron transfer between centres [8]. These data indicate, supporting previous data obtained with the porcine protein [5], that there is a single type of ubiquinone site per molecule of ETF-QO. ETF-QO has been shown to behave on non-denaturing electrophoresis as a monomer [6]. It seems unlikely that a dimer assembles to create a second quinone site. Finally, a preliminary structure determined by X-ray crystallography shows a single ubiquinone bound per monomer, and the compact structure of the protein seems to preclude an extensive conformational change to bring the cluster closer to the benzoquinone head group [4].

Comparing other quinone oxidoreductases with human ETF-QO, Warncke et al. [27] investigated the binding of shorter-chain ubiquinone homologues and corresponding 6-n-alkyl analogues by the Q_A and Q_B sites of the photosynthetic reaction centre from *Rhodobacter sphaeroides*. They showed that binding of the C-6 side chain is due primarily to the first two, and part of the third, isoprene groups, and that, unlike ETF-QO, the reaction centre exhibits a preference for the isoprene side chain over an n-alkyl side chain. Like ETF-QO, only the first three isoprene units of the quinone at the Q_A site make contact with the subunit [27,28]. Isoprene units four to ten extend into a crevice between the M and L subunits of the reaction centre. This previous work also indicated that it is the benzoquinone ring that provides most of the binding energy and suggested that the side chain is responsible for positioning the benzoquinone ring properly for efficient electron transfer in the reaction centre [27]. The quinone-binding sites in Complex I, NADH-ubiquinone oxidoreductase, and the *E. coli bo*-type ubiquinol oxidase have also been compared using ubiquinone

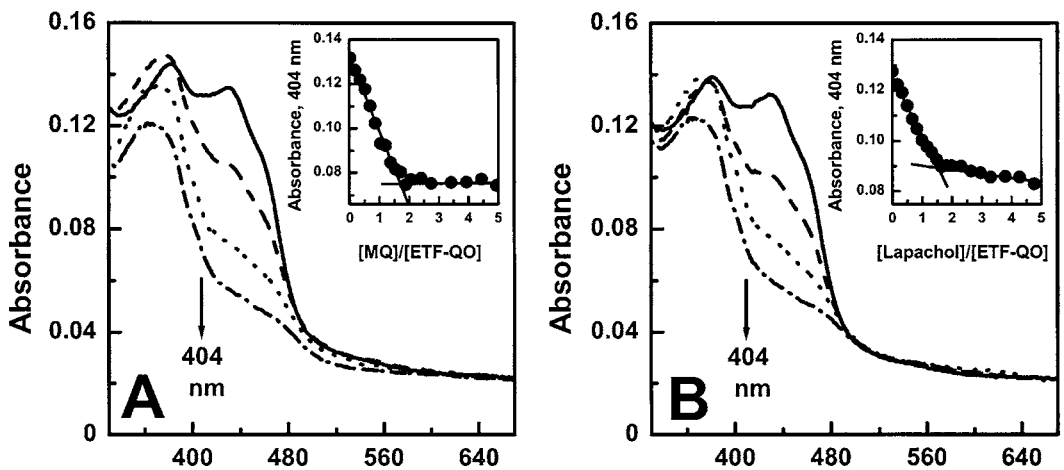

Figure 4 Reductive titration of human ETF-QO with menaquinol-1 (A) and lapachol (B) under anaerobic conditions

The reaction mixture containing human ETF-QO (5.6 μM) in 50 mM Hepes buffer, pH 7.4, containing 6 mM CHAPS and 30 mM glucose, was made anaerobic as described in the legend of Figure 1 and titrated with menaquinol-1 (MQ) (**A**) and lapachol (**B**). Stocks of 0.4 mM menaquinol-1 in 50 mM Hepes buffer, pH 7.4, containing 40 % ethanol and 6 mM CHAPS, and lapachol in 50 mM Hepes buffer, pH 7.4, containing 6 mM CHAPS were prepared by titration with sodium borohydride under strictly anaerobic conditions. The end of the reductive titration of the naphthoquinones was detected spectroscopically by measurement of the decrease in absorbance at 270 nm in the case of menaquinone-1 and at 278 (or 485) nm in case of lapachol. The reduced quinones were maintained under argon. The curves of absorbance spectra in the main plot of both quinones correspond to molar ratios of [quinol]/[ETF-QO] as follows: 0 (——), 0.5 (----), 1 (·····), and 1.5 (- - - - -). The insets show the decrease in absorbance at 404 nm as a function of the [quinol]/[ETF-QO] molar ratio. The absorbances at 404 nm in the inset correspond to the absorption spectra. All spectra were corrected for dilution and some spectra are omitted for clarity.

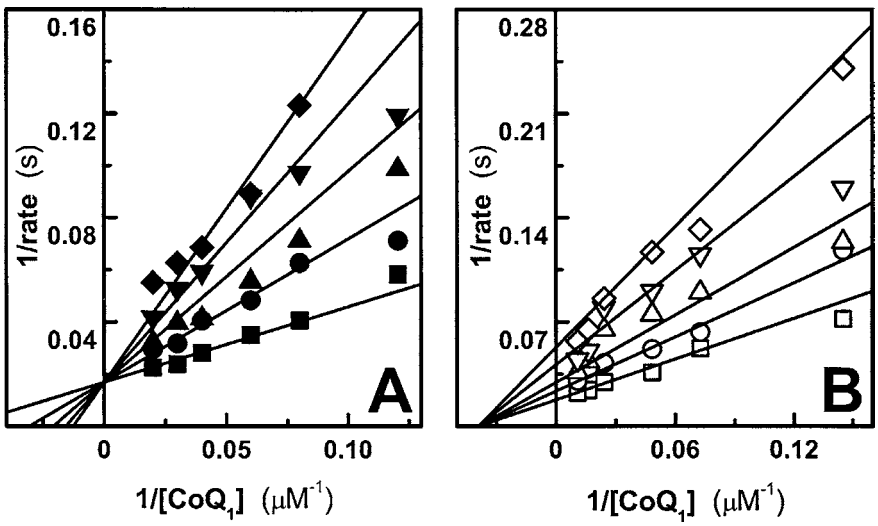

Figure 5 Inhibition of ETF-QO by HOQNO (A) and MPDNP (B) with CoQ_1 as the varied substrate

The data were analysed by non-linear least squares fit to equations for competitive and non-competitive inhibition. The activity of ETF-QO was measured at following concentrations of HOQNO: 0 (■), 25 (●), 50 (▲), 75 (▼) and 100 (◆) μM, and MPDNP: 0 (□), 1.5 (○), 3 (△), 6 (▽) and 9 (◇) μM. The final concentration of ethanol did not exceed 1 % (v/v) in the reactions.

analogues with variations in the side chain [29]. In Complex I, there is a very strong, but not absolute, requirement for the first methyl branch and the double bond in the first isoprene unit. In contrast, only one of the double bonds in the first two isoprene positions seems critical, and the enzyme does not discriminate between analogues with a methyl branch in these two positions. Finally, analysis of the donor ubiquinol site of Complex III using synthetic ubiquinone derivatives with alkyl side chains at C-6 showed that the decyl derivative supported the highest turnover [30]. The binding of shorter ubiquinone homologues and n-alkyl analogues by the bc_1 complex is also similar to that found with ETF-QO [26]. The binding constants for Q_1 and Q_3 (ubiquinone carrying a side chain of three isoprene units at the 6 position) are about 10 μM and 2 μM respectively, and the binding constant for decyl-ubiquinone is about the same as that of Q_2, 6 μM [26]. In the latter case, there seems to be no strong preference in the bc_1 complex for the isoprene side chain.

The k_{cat} of ETF-QO for 6-decylubiquinone, the synthetic derivate of CoQ with a ten-carbon-atom linear saturated alkyl substituent at C-6, is 84 % of that measured for CoQ_2, and the K_m for the decyl derivative is greater than the K_m for CoQ_2. This result would suggest that the methyl substituent or the relative rigidity of the isoprene is preferred in the binding site for the quinone side chain. Overall, these studies indicate that the quinone site of ETF-QO is similar with respect to the portion of the hydrocarbon side chain required for tight binding of the quinone. However, there seem to be differences with respect to the relative contributions of the isoprene side chain compared with an n-alkyl side chain.

Quinone analogue inhibitors of ETF-QO

Ubiquinone, plastoquinone and naphthoquinone analogues have proven useful in investigations of Complexes I, II and III of the respiratory chain and the quinone sites of the photosynthetic reaction centre. A number of these analogues were screened for their capacity to inhibit human ETF-QO at the K_m concentration of Q_1, 12 μM, and 10 and 100 μM inhibitor. Inhibitors of Complex I, including rotenone and pyridaben, had no effect on ETF-QO activity, i.e. $\leqslant 20$ % inhibition at 100 μM with Q_1 present at 12 μM, the K_m for this isoprenalogue [6]. No significant inhibition was given by antimycin A, stigmatellin or myxothiazole, inhibitors of Complex III, nor by carboxin, an inhibitor of Complex II. No inhibition was observed with a triazine inhibitor of photosystem II [31]. HOQNO, MPDNP and IDNP at 100 μM inhibited human ETF-QO by 62 %, 91 % and 33 % respectively. Inhibition by HOQNO and MPDNP was investigated in further detail. HOQNO, considered to be a naphthosemiquinone analogue [32–34], inhibits ETF-QO competitively with respect to Q_1 with $K_i = 27.8 \pm 3.0$ μM (Figure 5A). This compares with $K_i =$ 25 μM for fumarate reduction by succinic dehydrogenase and submicromolar K_i for succinate oxidation and fumarate reduction by menaquinol-fumarate oxidoreductase; both of the latter enzymes are inhibited non-competitively [35]. The level of inhibition by HNNQ was significantly less (33 %) in the preliminary experiments in which the concentration of Q_1 was 12 μM and the concentration of HNNQ was 100 μM. This suggests a narrow specificity for the alkyl side chain of these naphthoquinone analogues. Based on recent crystallographic studies of quinol-fumarate reductase, HOQNO and 2-[1-(*p*-chlorophenyl)ethyl]-4,6-dinitrophenol, block binding of menaquinone at the $Q_{P\,site}$ near the [3Fe–4S] cluster [36]. Both the competitive inhibition by HOQNO and the capacity to utilize menadione as an alternative substrate indicate that the quinone site of human ETF-QO can also accommodate naphthoquinones. Also, since the protein binds DBMIB, the data suggest that the protein must have a rather plastic site for binding the quinone head group.

MPDNP inhibited ETF-QO non-competitively with $K_i = 4.6 \pm$ 0.3 μM (Figure 5B). Although not investigated in detail, MPDNP also inhibits menadione reduction. The IC_{50} is 8 μM in the presence of 20 μM menadione, and inhibition of menadione reduction is non-competitive with $K_i \approx 20$ μM. 2-Substituted alkyl dinitrophenols have been characterized as inhibitors of quinone oxidoreductases in mitochondria and of photosystem II [37–39]. Inhibition by specific dinitrophenols of different quinone oxidoreductases has been related to the hydrophobicity of the side chain

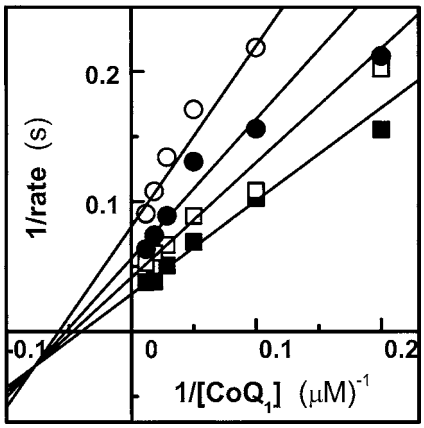

Figure 6 Inhibition of ETF-QO by PCP with CoQ_1 as the varied substrate

ETF-QO activity was determined in the presence of following concentrations of PCP: 0 (■), 3 (□), 7.5 (●) and 20 (○) μM. The final concentration of ethanol did not exceed 1 % (v/v) in the mixture.

at C-2 [40]. Based on the hydrophobicity index for 2-alkyl-4,6-dinitrophenol derivatives, the side chain of MPDNP is approx. 2-fold more hydrophobic than that of the 2-isopropyl derivatives that are relatively poor inhibitors [37]. A preliminary crystallographic study of pig ETF-QO [4], which is very similar to the human protein [41], suggests that the entrance to the ubiquinone site is buried in one hydrophobic side of the bilayer membrane that probably requires a hydrophobic entrance to the site. However, perhaps of greater significance is the fact that, based on molecular orbital calculations [37], the α-methyl substitution of IDNP orientates the three-carbon-atom side chain almost perpendicular to the phenol ring. This is not the case with MPDNP, in which the methyl substitution is β to the phenolic ring, greatly decreasing the interaction with the phenolic hydroxyl.

Pentachlorophenol is a simple non-competitive inhibitor of succinate-ubiquinone oxidoreductase and quinol-fumarate reductase with K_i values between 20 and 40 μM [35,40]. At 10 and 100 μM, ETF-QO activity was reduced by 44 and 89 % respectively, when assayed under the standard conditions described above. Inhibition of ETF-QO with varied Q_1 and PCP as the fixed, varied inhibitor was best-fitted to the equation describing mixed hyperbolic inhibition (Figure 6). In this analysis, K_i is 7.7 ± 2.6 μM, and the values of the constants, α and β, are 0.61 ± 0.23 and 0.20 ± 0.05, respectively. Therefore inhibition of human ETF-QO by PCP is more complex than inhibition by the other inhibitors described in the present paper, and more complex than PCP inhibition of other quinone oxidoreductases [35], because the inhibition may affect K_s, K_i, and k_{cat} [13].

Conclusions

The experiments of the present study support the contention that there is one quinone-binding site per ETF-QO monomer. This conclusion is based on observations of a single type of ubiquinone binding in the porcine and human ETF-QOs, the determination of simple steady-state kinetic patterns with a variety of ubiquinone homologues and analogues, the demonstration that the protein migrates as a monomer on non-denaturing gel electrophoresis [6], and a preliminary crystal structure that shows one equivalent of ubiquinone bound per monomer [4]. The ability to bind the quinone substrates, evaluated from the steady-state kinetic data, is correlated with the interaction of side chain with the protein that includes only the first two isoprene groups. The substrate-specificity observed with ubiquinone derivatives with isoprene and n-alkyl side chains and the susceptibility to known inhibitors of quinone oxidoreductases is consistent with the idea that the quinone sites in this group of proteins are very different, but similar in that shorter-chain homologues usually bind more tightly than those with longer side chains. The role of the 2-methyl branch and the double bond of the isoprene are usually confined to the first two isoprene groups, which probably orient the benzoquinone head group. The fact that CoQ_{10} is the physiologically relevant quinone in mitochondria probably reflects the requirement for ubiquinone to function as a mobile electron carrier in the biological membranes and, as Warncke et al. [26] point out, to prevent interference of quinone function by amphiphilic species present in native membranes. Overall, the strongest relationship between substrate structure and the catalytic efficiency of the enzyme, k_{cat}/K_m, is between the chain length of the substitution at the 6-position of the 1,4-benzoquinone and the structure of the binary complex that shows that only two isoprene units of the quinone actually interact with the protein [4]. Also, the specificity for binding most quinone inhibitors/toxins is extremely narrow. For the greatest part, the classical inhibitors of other quinone oxidoreductases do not inhibit ETF-QO. However, the 2-alkyl nitrophenol group of inhibitors initially demonstrated by Miyoshi and colleagues [37,38,42] as probes for quinone-binding sites may prove to be useful as specific inhibitors of ETF-QO given the limited results presented in the present paper. Since the three-dimensional structure should be available [4], it may be possible to design specific 2-nitrophenol inhibitors for ETF-QO. Finally, these experiments will support on-going investigations with site-directed mutations in the quinone-binding site of this iron–sulphur flavoprotein.

We thank Dr K. S. Rao and Mr Mark Albro for helpful criticisms. We are grateful to Dr Rona Ramsay and Dr Hideto Miyoshi for their assistance and Dr Bernard Trumpower for the gift of the ubiquinone analogues. This research was supported by a grant, HD 08315, from the National Institutes of Health.

REFERENCES

1 Frerman, F. E. (1988) Acyl-CoA dehydrogenases, electron transfer flavoprotein and electron transfer flavoprotein dehydrogenase. Biochem. Soc. Trans. **16**, 416–418
2 Frerman, F. E. (1987) Reaction of electron transfer flavoprotein ubiquinone oxidoreductase with the respiration chain. Biochim. Biophys. Acta **893**, 161–169
3 Frerman, F. E. and Goodman, S. I. (2001) Defects of electron transfer flavoprotein and electron transfer flavoprotein-ubiquinone oxidoreductase: glutaric acidemia type II. In The Metabolic and Molecular Bases of Inherited Disease (Scriver, C. R., Beaudet, A. L., Sly, W. S. and Valle, D., eds.), vol. II, 8th edn, pp. 2357–2365, McGraw-Hill, New York
4 Kim, J.-J. P., Zhang, J. and Frerman, F. E. (2002) Three-dimensional structure of porcine electron transfer flavoprotein-ubiquinone oxidoreductase. In Flavins and Flavoproteins 2002 (Chapman, S., Perham, R. and Scrutton, N., eds.), pp. 77–82, Rudolf Weber, Berlin
5 Watmough, N. J., Loehr, J. P., Drake, S. K. and Frerman, F. E. (1991) Tryptophan fluorescence in electron transfer flavoprotein-ubiquinone oxidoreductase. Biochemistry **30**, 1317–1323
6 Šimkovič, M., DeGala, G. D., Eaton, S. S. and Frerman, F. E. (2002) Expression of human electron transfer flavoprotein-ubiquinone oxidoreductase from a baculovirus vector: kinetic and spectral characterization of the human protein. Biochem. J. **364**, 659–667
7 Paulsen, K. E., Orville, A. M., Frerman, F. E., Lipscomb, J. D. and Stankovich, M. T. (1992) Redox properties of electron-transfer flavoprotein ubiquinone oxidoreductase as determined by EPR-spectroelectrochemistry. Biochemistry **31**, 11755–11761
8 Page, C. C., Moser, C. C., Chen, X. and Dutton, P. L. (1999) Natural engineering principles of electron tunneling in biological oxidation–reduction. Nature (London) **402**, 47–52
9 Yu, C. A. and Yu, L. (1982) Syntheses of biologically active ubiquinone derivatives. Biochemistry **21**, 4096–5101

10 Griffin, K. J., DeGala, G. D., Eisenreich, W., Mueller, F., Bacher, A. and Frerman, F. E. (1998) ^{31}P-NMR spectroscopy of human and *Paracoccus denitrificans* electron transfer flavoproteins, and ^{13}C- and ^{15}N-NMR spectroscopy of human electron transfer flavoprotein in the oxidized and reduced states. Eur. J. Biochem. **255**, 125–132
11 DuPlessis, E. R., Pellett, J., Stankovich, M. T. and Thorpe, C. (1998) Oxidase activity of the acyl-CoA dehydrogenases. Biochemistry **37**, 10469–10477
12 Ramsay, R. R., Steenkamp, D. J. and Husain, M. (1987) Reactions of electron-transfer flavoprotein and electron-transfer flavoprotein:ubiquinone oxidoreductase. Biochem. J. **241**, 883–892
13 Segel, I. H. (1975) Enzyme Kinetics: Behavior and Analysis of Rapid Equilibrium and Steady State Enzyme Systems, John Wiley & Sons, New York
14 Lakowicz, J. R. (1999) Principles of Fluorescence Spectroscopy, 2nd edn, Kluwer Academic/Plenum Publishing, New York
15 Lehrer, S. S. and Fasman, G. D. (1966) The fluorescence of lysozyme and lysozyme substrate complexes. Biochem. Biophys. Res. Commun. **23**, 133–138
16 Beckmann, J. D. and Frerman, F. E. (1985) Electron-transfer flavoprotein-ubiquinone oxidoreductase from pig liver: purification and molecular, redox, and catalytic properties. Biochemistry **24**, 3913–3921
17 Bradford, M. M. (1976) A rapid and sensitive method for the quantitation of microgram quantities of protein utilizing the principle of protein-dye binding. Anal. Biochem. **72**, 248–254
18 Wissenbach, U., Kroger, A. and Unden, G. (1990) The specific functions of menaquinone and demethylmenaquinone in anaerobic respiration with fumarate, dimethylsulfoxide, trimethylamine *N*-oxide and nitrate by *Escherichia coli*. Arch. Microbiol. **154**, 60–66
19 Petrova, S. A., Ksenzhek, O. S. and Kolodyazhnyik, M. V. (2000) Redox properties of naturally occurring naphthoquinones: vitamin $K_{2(20)}$ and lapachol. Russ. J. Electrochem. **36**, 767–772
20 Trebst, A., Harth, E. and Draber, W. (1970) On a new inhibitor of photosynthetic electron-transport in isolated chloroplasts. Z. Naturforsch. **25B**, 1157–1159
21 Lam, E. (1984) The effects of quinone analogues on cytochrome b_6 reduction and oxidation in a reconstituted system. FEBS Lett. **172**, 255–260
22 Degli Esposti, M., Rugolo, M. and Lenaz, G. (1983) Inhibition of the mitochondrial bc_1 complex by dibromothymoquinone. FEBS Lett. **156**, 15–19
23 Degli Esposti, M., Rotilio, G. and Lenaz, G. (1984) Effects of dibromothymoquinone on the structure and function of the mitochondrial bc_1 complex. Biochim. Biophys. Acta **767**, 10–20
24 Rich, P. R., Madgwick, S. A. and Moss, D. A. (1991) The interactions of duroquinol, DBMIB and NQNO with the chloroplast cytochrome *bf*-complex. Biochim. Biophys. Acta **1058**, 312–328
25 Rich, P. R. and Bendall, D. S. (1980) The kinetics and thermodynamics of the reduction of cytochrome *c* by substituted *p*-benzoquinols in solution. Biochim. Biophys. Acta **592**, 506–518
26 Samworth, C. M., Degli Esposito, M. and Lenaz, G. (1988) Quenching of the intrinsic tryptophan fluorescence of mitochondrial ubiquinol-cytochrome *c* reductase by the binding of ubiquinone. Eur. J. Biochem. **171**, 81–86
27 Warncke, K., Gunner, M. R., Braun, B. S., Gu, L., Yu, C. A., Bruce, J. M. and Dutton, P. L. (1994) Influence of hydrocarbon tail structure on quinone binding and electron-transfer performance at the Q_A and Q_B sites of the photosynthetic reaction center protein. Biochemistry **33**, 7830–7841
28 Allen, J. P., Feher, G., Yeates, T. O., Komiya, H. and Rees, D. C. (1987) Structure of the reaction center from *Rhodobacter sphaeroides* R-26: the protein subunits. Proc. Natl. Acad. Sci. U.S.A. **84**, 6162–6166
29 Sakamoto, K., Miyoshi, H., Ohshima, M., Kuwabara, K., Kano, K., Akagi, T., Mogi, T. and Iwamura, H. (1998) Role of the isoprenyl tail of ubiquinone in reaction with respiratory enzymes: studies with bovine heart mitochondrial complex I and *Escherichia coli bo*-type ubiquinol oxidase. Biochemistry **37**, 15106–15113
30 Yu, C. A., Gu, L. Q., Lin, Y. Z. and Yu, L. (1985) Effect of alkyl side chain variation on the electron-transfer activity of ubiquinone derivatives. Biochemistry **24**, 3897–3902
31 Lancaster, C. R. and Michel, H. (1999) Refined crystal structures of reaction centres from *Rhodopseudomonas viridis* in complexes with the herbicide atrazine and two chiral atrazine derivatives also lead to a new model of the bound carotenoid. J. Mol. Biol. **286**, 883–898
32 Smirnova, I. A., Hagerhall, C., Konstantinov, A. A. and Hederstedt, L. (1995) HOQNO interaction with cytochrome *b* in succinate:menaquinone oxidoreductase from *Bacillus subtilis*. FEBS Lett. **359**, 23–26
33 Rothery, R. A. and Weiner, J. H. (1996) Interaction of an engineered [3Fe–4S] cluster with a menaquinol binding site of *Escherichia coli* DMSO reductase. Biochemistry **35**, 3247–3257
34 Van Ark, G. and Berden, J. A. (1977) Binding of HQNO to beef-heart sub-mitochondrial particles. Biochim. Biophys. Acta **459**, 119–127
35 Maklashina, E. and Cecchini, G. (1999) Comparison of catalytic activity and inhibitors of quinone reactions of succinate dehydrogenase (succinate-ubiquinone oxidoreductase) and fumarate reductase (menaquinol-fumarate oxidoreductase) from *Escherichia coli*. Arch. Biochem. Biophys. **369**, 223–232
36 Iverson, T. M., Luna-Chavez, C., Croal, L. R., Cecchini, G. and Rees, D. C. (2002) Crystallographic studies of the *Escherichia coli* quinol-fumarate reductase with inhibitors bound to the quinol-binding site. J. Biol. Chem. **277**, 16124–16130
37 Saitoh, I., Miyoshi, H., Shimizu, R. and Iwamura, H. (1992) Comparison of structure of quinone redox site in the mitochondrial cytochrome-bc_1 complex and photosystem II (Q_B site). Eur. J. Biochem. **209**, 73–79
38 Tan, A. K., Ramsay, R. R., Singer, T. P. and Miyoshi, H. (1993) Comparison of the structures of the quinone-binding sites in beef heart mitochondria. J. Biol. Chem. **268**, 19328–19333
39 Yankovskaya, V., Sablin, S. O., Ramsay, R. R., Singer, T. P., Ackrell, B. A., Cecchini, G. and Miyoshi, H. (1996) Inhibitor probes of the quinone binding sites of mammalian complex II and *Escherichia coli* fumarate reductase. J. Biol. Chem. **271**, 21020–21024
40 Maklashina, E., Rothery, R. A., Weiner, J. H. and Cecchini, G. (2001) Retention of heme in axial ligand mutants of succinate-ubiquinone oxidoreductase (complex II) from *Escherichia coli*. J. Biol. Chem. **276**, 18968–18976
41 Goodman, S. I., Axtell, K. M., Bindoff, L. A., Beard, S. E., Gill, R. E. and Frerman, F. E. (1994) Molecular cloning and expression of a cDNA encoding human electron transfer flavoprotein-ubiquinone oxidoreductase. Eur. J. Biochem. **219**, 277–286
42 Sato-Watanabe, M., Mogi, T., Miyoshi, H., Iwamura, H., Matsushita, K., Adachi, O. and Anraku, Y. (1994) Structure–function studies on the ubiquinol oxidation site of the cytochrome *bo* complex from *Escherichia coli* using *p*-benzoquinones and substituted phonols. J. Biol. Chem. **269**, 28899–28907

Received 21 August 2003/28 October 2003; accepted 26 November 2003
Published as BJ Immediate Publication 26 November 2003, DOI 10.1042/BJ20031272